# Antenna array designing with an application for navigation landing of unmanned flying vehicle

Ivaylo Nachev[1] and Ilia Iliev[2]

*Abstract* – **This paper shows the examining of the design on the four-element antenna for pseudo-conical scanning with the application for navigation and inclusion to the landing of the unmanned aerial vehicle.**

*Keywords* – **phased-array antenna, electronic scanning antenna, pseudo–conical scanning, the orientation of unmanned aerial vehicles for automatic landing.**

## I. INTRODUCTION

With the entry of the unmanned aerial vehicles (UAV's) for various applications in the recent years, simulations and research results have emerged in scientific journals related to the automation of the process in the exploitation of the UAV. There are published different navigation and landing developments. Most of them are based on - differential GPS systems [1], pseudo-conical scanning [2], laser optical curtain [3], and landing site image recognition [4]. Some of these methods are designed with a big difference in landing area or they are expensive for realization.

This paper will consider the possibility to navigate and land of the UAV via a patch antenna array. As the main disadvantage of the pseudo-conical scanning [5] which is a problem can be the realization of the antenna and its high cost. The advantage of patch antenna arrays is their relatively small size, weight, and low cost. For this reason, this development can solve this problem.

## II. ANTENNA ARRAY DESIGN METHOD

An important step in designing a patch antenna is to choose a dielectric substrate on which patches are made. The employed substrate for the proposed design is Rogers RO4003 [6]. To increase the bandwidth and efficiency of the antenna "suspended substrate" is used [7], where the thickness of the gap between the ground plane and the antenna is Δ=1mm. In this method, we use the equivalent Dielectric constant (7). The operating frequency is chosen to be $fc$ = 10.525GHz, then wavelength λ = 28.50mm, and λg = 22.6150mm – the wavelength in the substrate. For calculation of the antenna dimensions, we are using the basic algorithm like in [8].

Step 1: Width (W) calculation: Width of the Microstrip antenna is given by the equation:

$$W = \frac{c}{2fc}\left(\frac{\varepsilon_r+1}{2}\right)^{-\frac{1}{2}} = 12.2mm, \frac{W}{h} > 1 \qquad (1)$$

Where c is the speed of the light c=3*10$^8$, $\varepsilon_r$ is a dielectric constant of the substrate, $fc$ is operation frequency and h is the substrate thickness.

Step 2: Effective Length ( $L_{eff}$) calculation: Length of the microstrip radiator is given by:

$$L_{eff} = \frac{c}{2fc\sqrt{\varepsilon_r}} = 11.3mm \qquad (2)$$

Where $\varepsilon_r$ is an effective dielectric constant of the substrate.

Step 3. Length extension ($L_{exp}$) calcualation: The actual length is obtained by the equation (accounting for the fringing fields):

$$L_{exp} = 0.412h\frac{(\varepsilon_{eff}+0.3)\left(\frac{W}{h}+0.264\right)}{(\varepsilon_{eff}-0.258)\left(\frac{W}{h}+8\right)} = 0.88mm \qquad (3)$$

Step 4: The actual length of the Patch (L) calculation: The actual length of the patch is given by:

$$L = L_{eff} + 2\,L_{exp} = 12.96mm \qquad (4)$$

Determination of effective dielectric permittivity $\varepsilon_{eff}$:

$$\varepsilon_{eff} = \frac{\varepsilon_r+1}{2} + \frac{\varepsilon_r-1}{2}\left(1+10\frac{h}{W}\right)^{0.5} = 1.58 \qquad (5)$$

The length of the guided wave:

$$\lambda g = \frac{\lambda}{\sqrt{\varepsilon_{eff}}} = 22.62 \qquad (6)$$

The influence of the gap is taken into account:

$$\varepsilon_{req} = \frac{\varepsilon_r(h+\Delta)}{(\varepsilon_r+h)\Delta} = 1.72 \qquad (7)$$

Where Δ is the thickness of the gap. The new dielectric constant in technology with the suspended substrate is $\varepsilon_{req}$=1.72, where the characteristics of the air are also taken into account.

In Table 1 are presented the values of one element from the antenna array. The simulation model of the antenna array structure is shown in Figure 1. Corporate feed network is used, thereby scanning is available in

[1]Ivaylo Nachev is a student at the Faculty of Telecommunications at the Technical University of Sofia, 8 Kl. Ohridski Blvd, Sofia 1000, Bulgaria, E-mail: ivaylonachev@yahoo.com

[2]Ilia Iliev, Professor at the Faculty of Telecommunications at the Technical University of Sofia, 8 Kl. Ohridski Blvd, Sofia 1000, Bulgaria, E-mail: igiliev@tu-sofia.bg

azimuth and elevations. The rounded edges of the square model of patch antenna provide circular polarization. It is important in navigation because there is interference between the antenna and the object sought. The antenna will not be able to detect the subject with ordinary linear polarization.

TABLE I
THE VALUES OBTAINED FOR THE DIMENSION OF THE ANTENNA COMPONENTS

| | W [mm] | $L_{eff}$ [mm] |
|---|---|---|
| Calculated | 12.2 | 23.96 |
| After simulation | 19.5 | 10.5 |

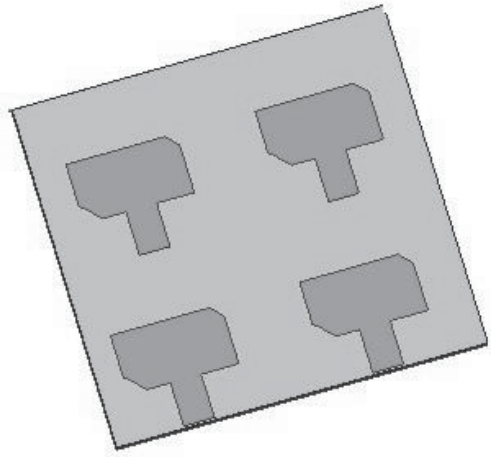

Fig. 1. Patch array 2x2 – simulation model

## III. TRANSMISSION LINES PHASE SHIFTER

The antenna feeder uses systems of connected microstrip lines (MS), delay lines (DL), T-junctions and quarter wave transformers in planar realization. The designed antenna is for realization with the pseudo-conical scanning. Pseudo-conical scanning is a method in which the antenna beam is shifted from its central axis. The beam has several states. Every state moves the beam away from the beam position from the previous one. The beam makes a whole circuit around the central axis. In our case - by sequentially changing these states, a flying device measure beams in different antennas states. When the signal levels of the four beams are equal, it is assumed that, that the device is in the center.

The designed antenna has five states – two states in azimuth, and two states in elevation, and one main state - the beam is the same as the center axis of the radiation. These are accomplished by increasing the electrical length by 90º of two patch elements using a delay line. Each of different beam has width 18º. Different beams are at a distance of 40º. The center of each beam is offset at 20º from the central axis.

Figure 2 shows the block diagram of the feeder network. The antenna is supplied on feed point, then through the system made up of microwave elements, divided into four equal parts - 1/4 in each antenna. The control between diverse states of the antenna beams is performed by the switches represented in the block diagram. For this purpose, it is appropriate to use it is a PIN switch – instead of one diode, two diodes sequentially connected. This increase isolation. The high isolation is necessary, because of the high operating frequency is used. This way avoids unwanted reflections and drops in the effect of the antenna. [9]

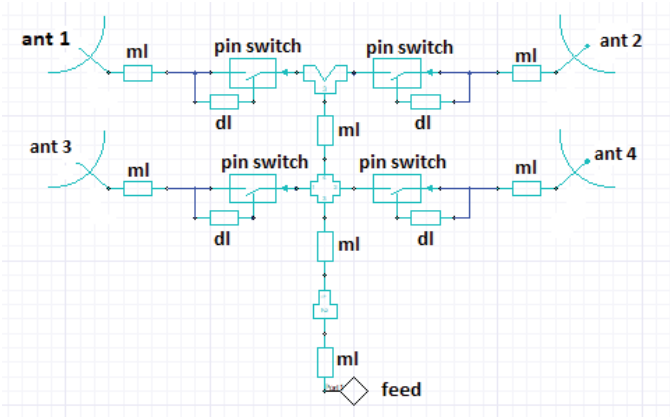


Fig. 2. Block diagram of feeder antenna network

## IV. SIMULATIONS RESULT

The next figures show the results of the simulations. In Fig. 3 is displayed the return loss of each segment of the antenna. The figure shown that each patch has a level S11 > - 15dB, for the operation frequency. From this value follows that the VSWR of each antenna element meets the requirement for high antenna efficiency. Table 3 shows the S11 and VSWR of each antenna element in the array. Figure 4 shows the return loss on antenna array inputs, after connecting the array and the feeder network. The figure shows that S11 = - 27.5dB. By using the formula VSWR = (1+S11) / (1-S11) [10], we get the value VSWR = 1.07, from which it follows that the losses in the antenna will not be bigger than Mismatch loss = 0.004dB and return power <0.10% [11].

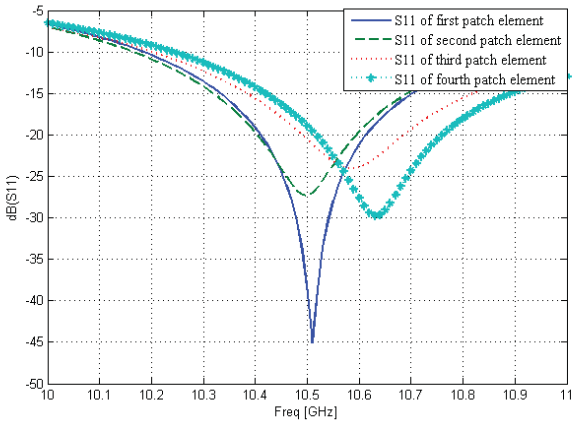


Fig. 3. Antenna bandwidth (S11)

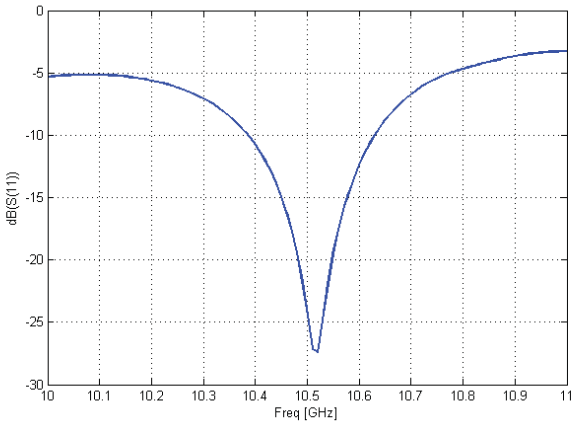


Fig. 4. Antenna bandwidth on feeder network inputs (S11)

TABLE II
VSWR IN DIFFERENT ANTENNA STATES

| | S11 [dB] | VSWR |
|---|---|---|
| First antenna element | -45.13 | 1.04 |
| Second antenna element | -28.32 | 1.07 |
| Third antenna element | -20.69 | 1.10 |
| Fourth antenna element | -19.55 | 1.11 |

Figure 5 shows the antenna radiation pattern in case 1 whit Gain = 12dB. To calculate the antenna coverage distance, the gain and the width of the beam plot are generally -3dB from the main peak [12]. In this case gain $GAcase_1 = 12 - 3 = 9dB$, whit the width of the beam = 20°. Taking the gain in each beam in scanning mode, shown in figure 6 and 7, respectively, are shown the two options of the antenna beam in azimuth and two in elevation. Each beam of the antenna has the same gain as case 1. The width of each the beam = 20°, the distance between the centers of the individual beams is 40°. The center of each beam is offset at 20° from the central axis.

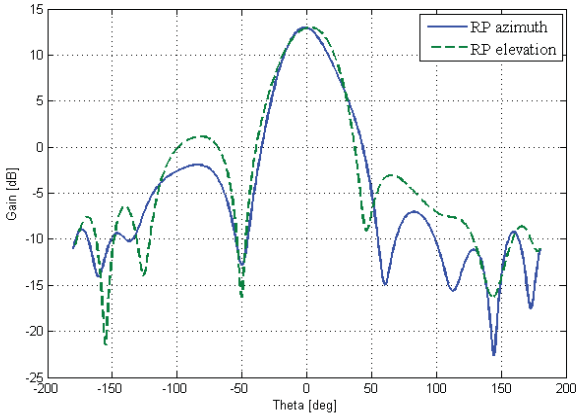


Fig. 5. Radiation pattern in case 1

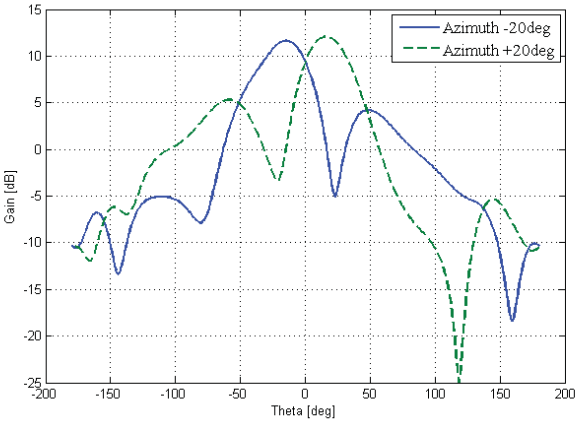


Fig. 6. Radiation pattern - two cases in azimuth

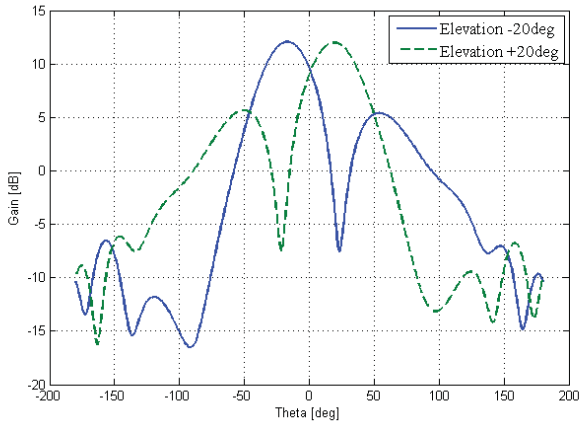


Fig. 7. Radiation pattern - two cases in elevations

## V. Conclusion

The main advantages of this proposed antenna are:

- easy control with a microcontroller;
- small sizes;
- low cost.

This antenna can be used for various applications for automatic landing and control of the landing of unmanned aerial vehicles on a ground or mobile landing site. Also, this type of antennas can be used with various applications in radio navigation, robotics, and automation of production processes.

The designed antenna is suitable for integration into a landing site of the UAV, whit a modified pseudo-conical scanning method. The targeting of UAV to the landing site can be performed on its GPS-coordinates for civilian purposes. Because the GPS position error is very large, the beams of the diagram of the antenna array cover the area in which the drone is localized (a cylinder of wrong positioning). When UAV get position in the center of the landing site, by measuring the levels of the different antenna beams in scanning mode, the UAV can start landing. Thus, the landing pad may have dimensions commensurate with the gauge of the UAV.

## References

[1] https://www.u-blox.com/en/product/c94-m8p#tab-documentation-resources

[2] Andreev K., Stanchev G., “Flight Safety Sensor and Auto-Landing System of Unmanned Aerial System”, Int. J. of Reasoning-based Intelligent Systems (IJRIS), Japan, 2019.

[3] Arnaudov R., Botusharov V., Stanchev G., Andreev K., "System for Automatic Targeting of Unmanned Aerial Vehicles in Vertical Landing ", Patent Application No. 112876, Bulgarian Patent Office, February 2019, Sofia.

[4] Fumio Ohtomo, Kazuki Osaragi, Tetsuji Anai, Hitoshi Otani, US Grant Patent number US20120277934A1, “Taking-Off And Landing Target Instrument And Automatic Taking-Off And Landing System”, 2011.

[5] Andreev K., "Improvement of functional parameters on control systems of unmanned aerial vehicles", Ph.D. Thesis Dissertation, TU-Sofia, Bulgaria, 2019.

[6] Prabhakaran. M, Veeramani. R, 2015, “Comparative Analysis of Microstrip Phased Array Antenna Design”, International Journal of Advanced Information Science and Technology (IJAIST), Vol.4, No.2, February 2015, ISSN: 2319:2682, DOI:10.15693/ijaist/2015.v4i2.306-310

[7] Rogers RO4003 specification: https://www.rogerscorp.com/documents/726/acm/RO4000-Laminates---Data-sheet.pdf

[8] Chang, Kai; "RF and Microwave Wireless Systems", 2000, ISBN: 0-471-35199-7.

[9] Arnaudov. R, Stanchev G., Andreev K., " System for automatically targeting of unmanned aerial vehicle with vertical landing on mobile landing site", 54th International Scient. Conference on Information, Communication and Energy Systems and Technologies, Ohrid, Republic of North Macedonia, June 27-29 2019.

[10] Balanis A. Constantine, Antenna Theory: Analysis and Design, 3rd Edition, ISBN-13: 978-0471667827

[11] https://www.markimicrowave.com/blog/wp-content/uploads/2016/11/return-loss-to-vswr.pdf

[12] http://www.rfwireless-world.com/calculators/Antenna-Range-Calculator.html